

---

# INTERNATIONAL JOURNAL OF CURRENT RESEARCH IN CHEMISTRY AND PHARMACEUTICAL SCIENCES

(p-ISSN: 2348-5213; e-ISSN: 2348-5221)

[www.ijcreps.com](http://www.ijcreps.com)

(A Peer Reviewed, Referred, Indexed and Open Access Journal)

DOI: 10.22192/ijcreps

Coden: IJCROO(USA)

Volume 11, Issue 3- 2024

---

## Research Article



DOI: <http://dx.doi.org/10.22192/ijcreps.2024.11.03.005>

## Silver Nanoparticles (AgNPs) characterization of antibacterial and antioxidant properties using *Myristica fragrans* ethanol extract

**B. Praveen<sup>1</sup>, R. Manikandan<sup>2\*</sup>, M. Surendra Varma<sup>2</sup>, G. Anburaj<sup>2</sup>,  
D. Chinnaraja<sup>2</sup>, C. Sathish Prabu<sup>3</sup>, M. Revathi<sup>4</sup>**

<sup>1</sup>P.G scholar, Department of Chemistry, PRIST Deemed to be University Thanjavur.

<sup>2</sup>Department of Chemistry, PRIST Deemed to be University Vallam, Thanjavur.

<sup>3</sup>Department of Chemistry, Kuppam Engineering College, Chittur(Dt) Andra Pradesh

<sup>4</sup>Department of Chemistry, Adhiparasakthi Group of Institutions, Melmaruvathur.

Corresponding Author Email.ID: [marksian22@gmail.com](mailto:marksian22@gmail.com)

---

### Abstract

(AgNPs) Silver Nanoparticles synthesised from the ethanol extract of *Myristica fragrans* seed was employed for the removal of the Rhodamine B. The adsorbents were characterised by UV-Visible, FT-IR, XRD, SEM, TEM and AFM. Silver Nanoparticles showed significant antibacterial and DPPH Radical Scavenging Assay action on both the gram classes of gram negative *Escherichia coli* and gram negative bacteria *Bacillus cereus*.

**Keywords:** *Myristica fragrans*, FT-IR, XRD, SEM, TEM, AFM rhodamine B, DPPH Radical Scavenging Assay.

---

### I. Introduction

Plants have been used in virtually all cultures as a source of medicine. Plants have provided a source of inspiration for novel drug compounds, as plant-derived medicines have made large contributions to human health and well-being (Anburaj et al. 2016). The enormous surge in multi-drug-resistant pathogens has emerged as a vital

challenge for scientists to develop effective therapeutics. Particles with a size range of 1–100 nm are considered nanoparticles (NPs), and silver nanoparticles (AgNPs) have been highly effective antimicrobial agents (Vidyasagar et al., 2023). In the present study, mace-mediated silver nanoparticles (mace-AgNPs) were synthesized,

characterized, and evaluated against an array of pathogenic microorganisms. Mace, the arils of *Myristica fragrans*, are a rich source of several bioactive compounds, including polyphenols and aromatic compounds (Rizwana et al., 2021). Researchers are very interested in noble metal nanoparticles among all nanomaterials because noble metals have various potential applications in the fields of physics, materials science, biology, chemistry, and medicine (Ohiduzzaman et al., 2024). Silver nanoparticles have been considered a major topic of research due to their distinct and strong plasmon resonance in the visible range, as well as their application in biological sciences. Metal nanoparticles are intriguing due to their simplicity of manufacturing and modification, as well as their size, shape, and dispersion (Jan et al., 2021). Silver nanoparticles (AgNPs) using two different extracts (aqueous and ethanolic) of *Tagetes erecta* flowers. When exposed to different biocompounds found in the plant, silver ions are reduced, thus resulting in the green synthesis of nanoparticles. After performing the optimization of synthesis, the obtained AgNPs were characterized using various techniques (Burlec et al., 2022).

## II. Materials and Methods

Materials – Freshnuts of *Myristica fragrans* was procured from a local supermarket. The Silver nitrate was supplied by Sigma Alrich Chemicals. All the Chemicals and Reagents were of Analytical grade.

### 2.1 Preparation of *Myristica fragrans* seed extract

We gathered the *Myristica fragrans* seeds from a nearby mega store. After being thoroughly cleaned with distilled water, the seeds were allowed to dry on their own. The seeds were moved from air drying to an ethanol-filled round-bottom flask. The mixture was refluxed for one to two hours, or until the alcoholic solution became yellow instead of colourless. Then the mixture was cooled at room temperature and filtered using Whatmann No.1 filter paper. The extract was stored in refrigerator for overnight.

### 2.2 Synthesis of Silver Nanoparticles

10 ml (0.1mM) Silver nitrate was treated with 5 ml of *Myristica fragrans* alcoholic seed extract and stirred at 65<sup>0</sup>C for 15 – 20 minutes. Color change from pale yellow to dark brown precipitate was observed. The brown precipitate was washed with ethanol several times. Then the precipitate was dried at 60<sup>0</sup>C in vacuum oven and stored in a sealed bottle (Ansari et al. 2023).

### 2.3 Characterisation of Silver Nanoparticles

#### 2.3.1 UV-Visible Spectral Analysis

The synthesised Silver Nanoparticles were characterised using Shimadzu UV 2450 Spectrophotometer.

#### 2.3.2 XRD

The XRD Spectrun of powdered sample of Silver Nanoparticles was obtained using a Philips P W 1710 diffractometer ( $\lambda = 0.15405 \text{ \AA}$ ) with monochromatized Cu K radiation source. The diffractogram was then compared to diffraction data in well –known database to determine what species exist in a sample (Goudarzi et al. 2016).

#### 2.3.3 FT-IR

The FTIR spectra of Silver Nanoparticles was recorded using Bruker model from 4000-400  $\text{cm}^{-1}$  by mixing dried sample with KBr pellets.

#### 2.3.4 SEM

The Surface Morphology of Silver Nanoparticles was identified by Scanninf Electron Microscope.

#### 2.3.5 AFM

The Surfacr Morphology of Silver Nanoparticles was analysed using Nanosurf easy scan 2 AFM in non-contact mode. Amplitude frequency was around 350 KHz, the mean length 120 nm and tip end diameter 10-15 nm.

### 2.3.6 Adsorbate Preparation

Rhodamine B supplied by BPH was used to investigate the adsorptive properties of the

adsorbents prepared. Table 1 shows the properties of Rhodamine B and Figure 1 shows the structure of Rhodamine B in its cationic and zwitter ionic forms (Al-Kahtani 2017).

Table 1 Properties of Rhodamine B

| Parameters        | Values   |
|-------------------|--|
| Suggested name    | Rhodamine B  |
| C.I number        | 45170  |
| C.I name          | Basic violet 10  |
| Class             | Rhodamine  |
| $\lambda_{max}$   | 554 nm   |
| Molecular Formula | C <sub>29</sub> H <sub>31</sub> N <sub>2</sub> O <sub>3</sub> Cl |
| Formula Weight    | 479.02   |

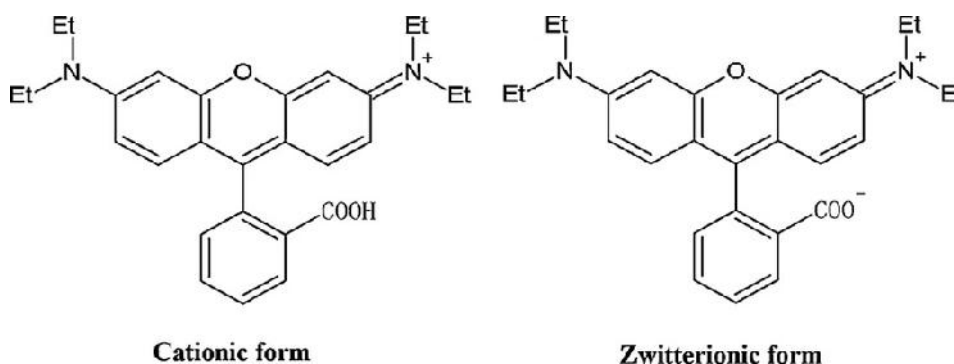


Figure 1 Structures of Rhodamine B

### 2.3.7 Batch Adsorption Experiments

Batch adsorption studies with respect to influence of adsorbent dosage, initial dye concentration, contact time and pH were carried out. The batch adsorption studies were performed by adding a fixed amount of adsorbent into a number of 250 ml Erlenmeyer flasks containing 20 – 80 mg/L of dye solution at a temperature of 25°C. The flasks were placed on a rotator shaker and agitation was provided at 180 rpm. The dye concentrations were measured at equilibrium. The amount of Rhodamine B adsorbed per unit mass of the adsorbent was determined by using the following equation

$$q_e = [C_0 - C_e / W] \times V \quad (2)$$

$$\% \text{ Removal} = [ [C_0 - C_e / C_0 ] \times 100 \quad (3)$$

Where,  $C_0$  is the initial Rhodamine B dye concentration in solution (mg/L),  $C_e$  is the equilibrium concentration in solution (mg/L), and  $V$  is the volume of the solution (L), and  $M$  is the mass of adsorbent used (g).

### 2.3.8 Antibacterial Activity

Antibacterial activity of Silver Nanoparticle against gram negative *Escherichia coli* and gram positive bacteria *Bacillus cereus* were observed using a agar well diffusion & disk diffusion method respectively. Mueller Hinton agar was prepared, sterilised and kept ready in molten condition. Various fractions of Silver Nanoparticles loaded discs were dispersed on the solidified Mueller Hinton agar with test organisms and standard organism. The plates were incubated at 37°C for 24 hours. MIC was recorded based on the growth of the organism.

### 2.3.9 DPPH Radical Scavenging Assay

The antioxidant assay of CuNPs from plants was used against DPPH radical and was determined by UV spectrophotometry at 517 nm. This activity was measured according to the method previously performed. Five different concentrations (100–500 µg/ml) of plant extracts were prepared. Ascorbic acid was used as a standard. 1 ml of each extract and 3 ml of each solvent were mixed with 0.5 ml of 1.0 mM DPPH in methanol and allowed to react at room temperature for 30 minutes. The same amount of solvent and DPPH are used to prepare the blank solution, which is a control. The sample was prepared in triplicate for each analysis, and the mean value of the absorbance was noted. The DPPH radical scavenging was calculated by the following formula:

**DPPH inhibition percentage**  

$$= [(A_0 - A_1) / A_0] \times 100$$

Where, A<sub>0</sub> - Absorbance of the control, A<sub>1</sub> - Absorbance of the CuNP/ascorbic acid.

The inhibitory concentration (IC<sub>50</sub>) of the plant extract was reported as the number of antioxidants required to reduce the initial DPPH concentration by 50%. A triplicate test was performed and graphs were plotted using the average of three determinations (Devika et al. 2023).

## III. Results and Discussion

### 3.1 Visual Confirmation/ UV-spectroscopy

Color change from pale yellow to brown when ethanol extract of *Myristica fragrans* was added drop wise to Silver nitrate formed the primary evidence for the formation of Silver Nanoparticles. (Fig. 2) This is in good agreement with the report of green synthesis of silver nanoparticles by *Aegle marmelos* leaf extract.

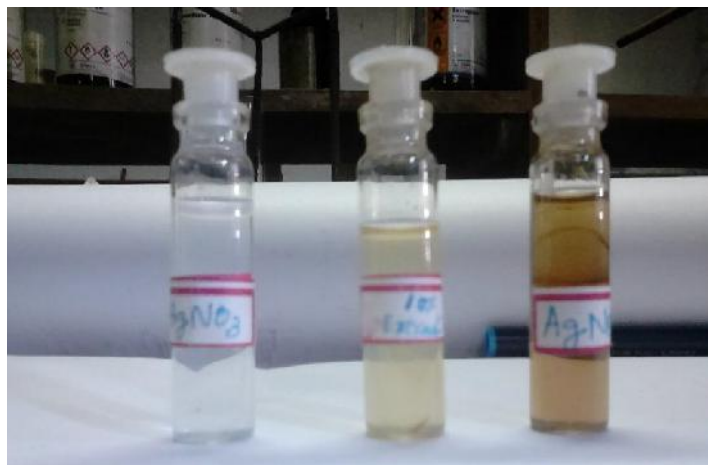


Fig.2 Color change of leaf extract from yellow (without silver nitrate) to brown (with silver nitrate)

The optical study is the best way to confirm the synthesis of nanoparticles. The Ag solution was optically analyzed by UV visible spectroscopy of range 200e800 nm at time interval of 40 min and

72 h as shown in figure 3. A strong characteristic peak of surface resonance of Ag nanoparticles was observed around 425 nm (Fatimah 2016).

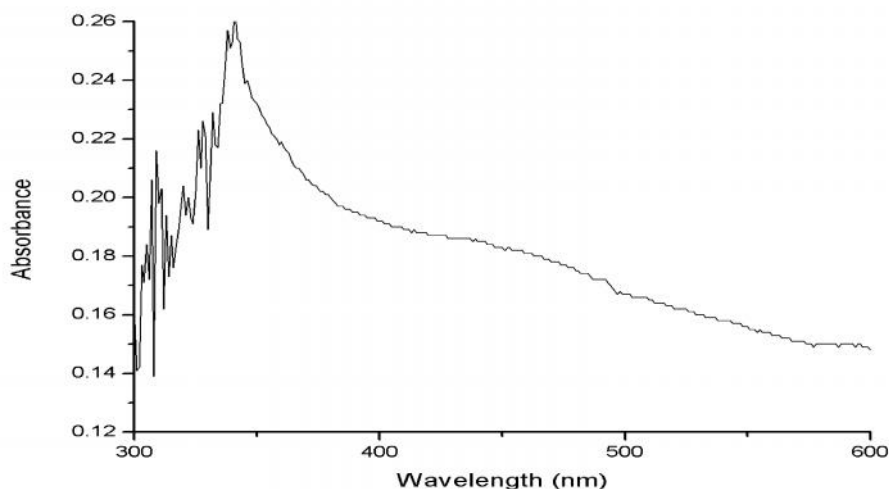


Fig. 3 UV-Visible spectrum of AgNPs

### 3.2 FTIR

The FT-IR Spectrum images of Silver Nanoparticle using ethanol extract of *Myristica fragrans* were recorded and shown in Fig. 4. The peaks at 3344, 2923  $\text{cm}^{-1}$  is due to the  $-\text{OH}$  stretching vibrations of phenols. Peaks corresponding to the wave numbers 2853, 1741 and 1382  $\text{cm}^{-1}$  shows the presence of C-H stretching. Wave numbers corresponding to 1242, 1097, 987 and 723  $\text{cm}^{-1}$  confirms the presence of aromatic hydrocarbons. In addition to that, peak corresponding to 1741  $\text{cm}^{-1}$  confirms the presence of aldehyde groups in the ethanol extract of *Myristica fragrans* which is responsible for the

capping and stabilization of biosynthesised Silver Nanoparticles. The purity of the synthesized NPs was checked by using FTIR spectroscopy within the range of 500-4000  $\text{cm}^{-1}$ . (Jan et al. 2021) FTIR spectra of pulp power and the biosynthesized AgNPs. FTIR spectra of pulp extract revealed peaks at 3290, 2924, 1640, 1340, 1000, 854, and 570  $\text{cm}^{-1}$  for the presence of different functional groups, which can play a significant role in the biosynthesis of metal or semiconductor oxide nano-particles. The stretching of the hydroxyl group ( $-\text{OH}$ ) from phenols and alcohols is responsible for the peak at wave number 3290  $\text{cm}^{-1}$  (Ohiduzzaman et al. 2024)

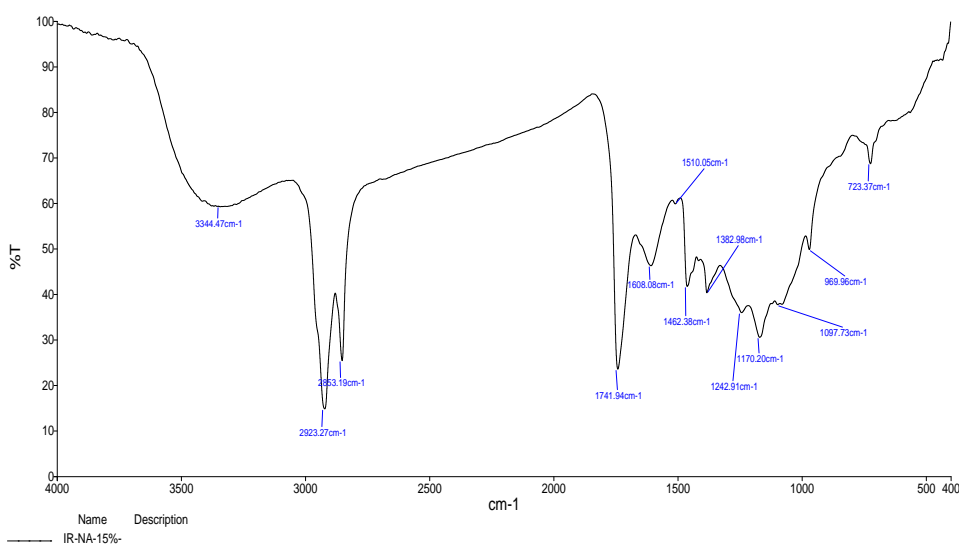


Fig.4 FT-IR Spectrum of AgNPs

### 3.3 XRD Pattern of AgNPs

Fig. 5 shows the XRD pattern of the synthesised Silver Nanoparticles using Cu K radiation source. ( $\lambda = 0.15405 \text{ \AA}$ ). All the different peaks can be well indexed to the orthorhombic structure of Silver Nanoparticles with lattice constant of  $a = 4.689 \text{ \AA}$ . Three intense peaks at  $2\theta = 37.94^\circ$ ,  $45.98^\circ$  and  $64.17^\circ$  corresponding to (123), (312) and (404) planes respectively confirmed orthorhombic structure (JCPDS-84-0713) of Silver Nanoparticles. The average size of Silver Nanoparticles was calculated using Debye-Scherrer's equation by determining the full width

at half maximum and found to be approximately  $\sim 10 \text{ nm}$ . In the XRD pattern, the three diffraction maxima at  $2\theta = 38.20^\circ$ ,  $44.30^\circ$ , and  $64.58^\circ$  were observed. The diffraction maxima were indexed as (111), (200), and (222) plane of the face center cubic structure of Ag. Wisam et al.<sup>47</sup> reported that peaks at  $2\theta = 38.20^\circ$ ,  $44.40^\circ$ , and  $64.60^\circ$  are typical diffractions of face-centered cubic (FCC) structured Ag (JCPDS Card no. 04-0783). Additional unassigned peaks (marked stars) appeared in the recorded XRD pattern due to the presence of bioorganic or metalloproteins in the solution (Hussain et al. 2023).

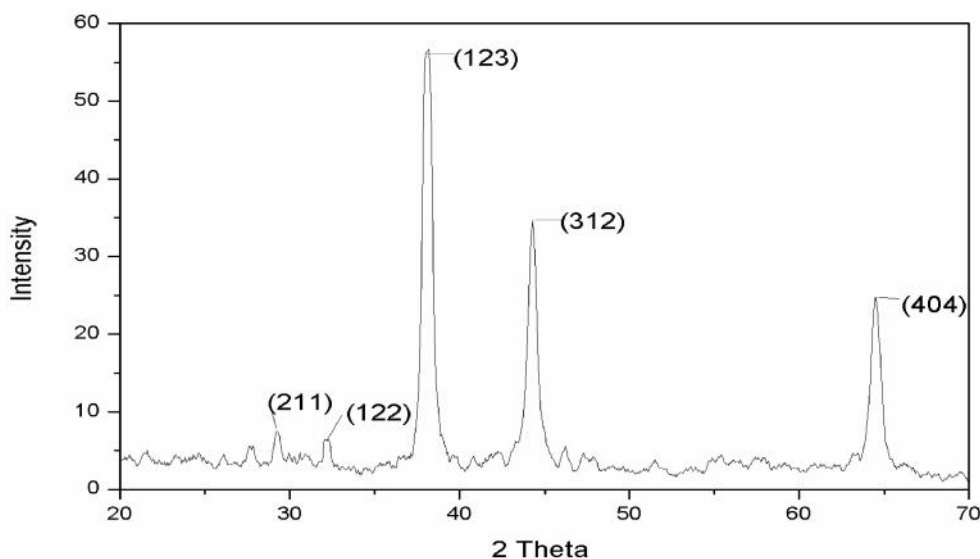


Fig. 5 XRD Pattern of AgNPs

### 3.4 SEM

SEM image of the Silver Nanoparticles were recorded and are shown in Fig. 6. SEM micrograph showed that the Silver Nanoparticles formed were uniform and crystalline with diameter range  $\sim 10 \text{ nm}$ . This result is in good agreement with the crystallite size calculated using the XRD data. Fig. 5 also reveals no

characteristic peaks of impurities or other precursor compounds are observed. SEM analysis indicated that the Ag-NPs were small, spherical to square shaped and found in agglomerated form. Analysis using dynamic light scattering indicated that these particles were of the sizes ranging from 40-70 nm (Thiyagarajan and Kanchana 2022).

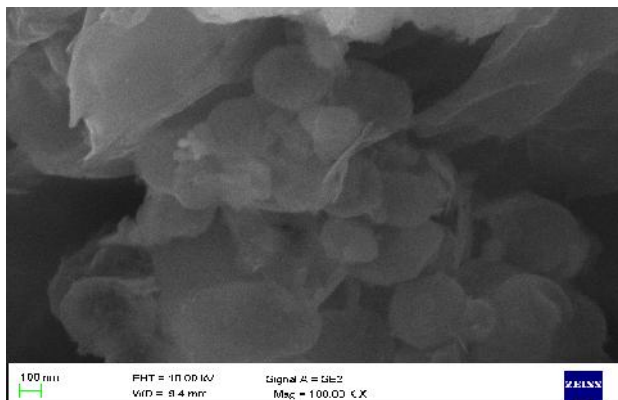


Fig. 6 SEM image of AgNPs

### 3.5 AFM

Fig. 7 shows the surface topography of Silver Nanoparticles synthesised using ethanol extract of

*Myristica fragrans* seeds. AEM images of Silver Nanoparticles exhibit uniformly distributed, well defined regular nanostructures.

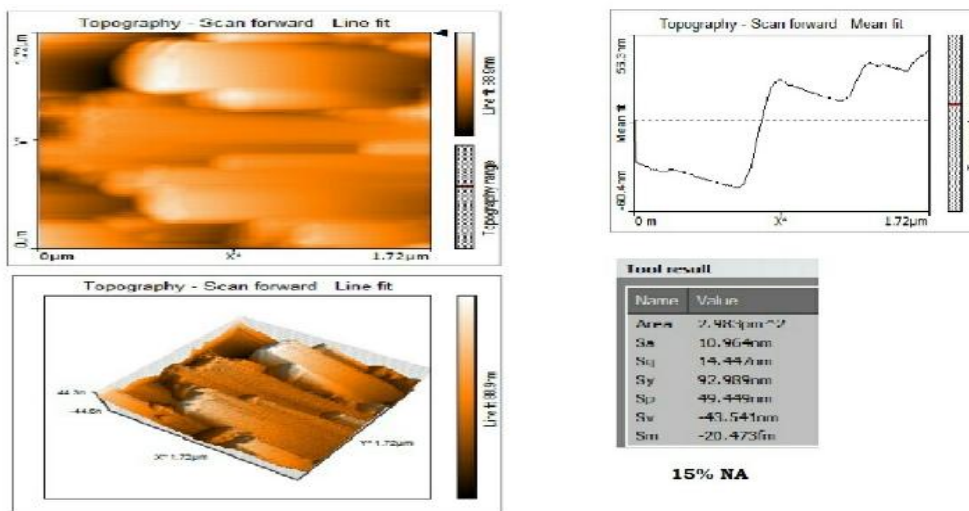


Fig.7 AFM image of AgNPs

### 3.6 Antibacterial Activity

Nanoparticle synthesis by green route are found to be highly effective against multi-drug resistant human pathogenic bacteria. Antibacterial activity of Silver Nanoparticles against *Escherichia coli* and *Bacillus cereus* were observed and compared. As the concentration of Silver Nanoparticles increases the zone of inhibition also increases. The maximum activity was found to be 35mm and 30mm for 400mg gram of both negative and

350mg of gram positive respectively. The antibacterial activity has been calculated by measuring the zone of inhibition and listed in Table 2. It was also observed that there was no zone of inhibition in the control (*Aloe vera* plant extract and silver nitrate solution) figure no. (8-10) and antibiotic discs viz. streptomycin, Ampicillin/Cloxacillin, Amikacin, Norfloxacin & Nitrofurantoin showed standard zone of inhibition against the same bacteria.(Chikdu; et al. 2015)

Table 2 Zone of Inhibition observed for *Escherichia coli* and *Bacillus cereus*

| AgNPs (mg) | Gram Negative Bacteria<br><i>Escherichia coli</i> (mm) | Gram Positive Bacteria<br><i>Bacillus cereus</i> (mm) |
|------------|--|---|
| 50         | 22   | 20  |
| 100        | 25   | 25  |
| 150        | 28   | 30  |
| 200        | 29   | 32  |
| 250        | 30   | 30  |
| 300        | 30   | 27  |
| 350        | 30   | 34  |



Fig. 8 Zone of Inhibition of AgNPs for gram negative bacteria *Escherichia coli*



Fig. 9 Zone of Inhibition of AgNPs for gram positive bacteria *Bacillus cereus*

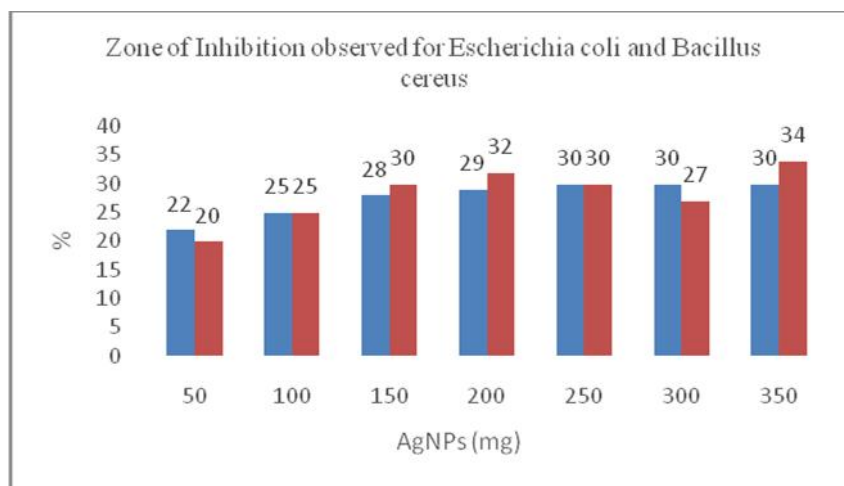


Fig. 10 Zone of Inhibition of AgNPs for gram positive bacteria *Bacillus cereus*



### 3.7 DPPH radical scavenging activity

These secondary metabolites can act as free radicals scavengers/inhibitors, which inactivates the antioxidants and repairs the oxidative stress caused by damage (Narayanan et al. 2023). A range of cell biomolecules, such as DNA, polypeptides and membrane lipids, might experience oxidative injury resulting from high oxidative stress brought on by the deed of “mitochondria” and other internal or external

causes. This deterioration can result in neurodegenerative disorders and senescence. IC<sub>50</sub> value 40.51 (μg/ml) Standard ascorbic acid 34.89 (μg/ml) show in the Fig;11 DPPH radicals react with suitable reducing agent as a result of which electron become paired off forming the corresponding hydrazine. The solution therefore loses color stoichiometrically depending on the number of electrons consumed which is measured spectrometrically at 517 nm (Perumal et al. 2010).

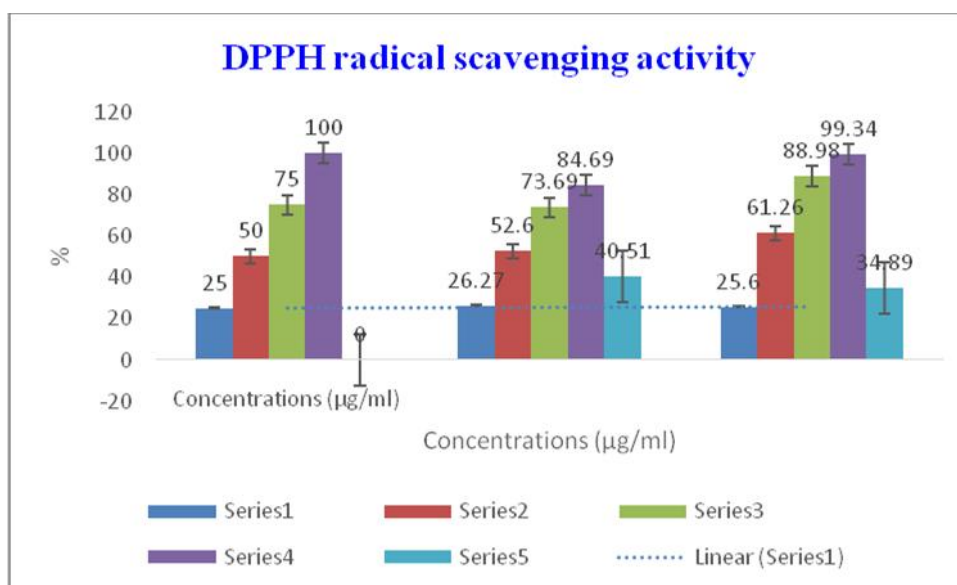


Fig. 11 Zone of Inhibition of AgNPs for gram positive bacteria *Bacillus cereus*

## V. Conclusion

AgNPs were prepared by the ethanol extract of *Myristica fragrans* seeds. The synthesized AgNPs were characterized with UV-Visible Spectroscopy, FT-IR, XRD, SEM and AFM studies. DPPH scavenging property compared to other extracts and standard. The new adsorbent have been applied for the removal of Rhodamine-B in batch sorption and the influence of parameters such as adsorbent dosage, contact time, initial dye concentration and pH was investigated. Analysis of experimental data of Langmuir, Freundlich and Temkin isotherm show that the equilibrium data were best fitted. Values of RL and the correlation coefficient showed that the Langmuir was the best fit model among the various isotherms. Thermodynamic parameter

$G^{\circ}$  was calculated and it was found to be -15.478 KJ/mol revealed that the removal process is spontaneous and of physisorption nature. The performance of AgNPs indicates that it can be used as an efficient adsorbent for removal of Rhodamine-B present in textile effluent.

## Acknowledgments

The founders have nothing but praise for the professionals and specialized personnel at PRIST University, for giving them a location to work. I'm writing to thank my superior for his advice, helpful recommendations, and invigorating clarifications.

## Conflicts of interest

The authors declare no conflict of interest.

## References

- Al-Kahtani, Abdullah A. 2017. "Photocatalytic Degradation of Rhodamine B Dye in Wastewater Using Gelatin/CuS/PVA Nanocomposites under Solar Light Irradiation." *Journal of Biomaterials and Nanobiotechnology* 08(01): 66–82. doi:10.4236/jbmb.2017.81005.
- Anburaj, G, M Marimuthu, V Rajasudha, and Dr R Manikandan. 2016. "Phytochemical Screening and GC-MS Analysis of Ethanolic Extract of *Tecoma stans* (Family: Bignoniaceae) 'Yellow Bell Flowers.'" *Int. J. of Res. in Pharmacology &Pharmacotherapeutics* 5(3): 256–61. www.ijrpp.com.
- Ansari, Madeeha, Shakil Ahmed, Asim Abbasi, Muhammad Tajammal Khan, Mishal Subhan, Najat A. Bukhari, Ashraf Atef Hatamleh, and Nader R. Abdelsalam. 2023. "Plant Mediated Fabrication of Silver Nanoparticles, Process Optimization, and Impact on Tomato Plant." *Scientific Reports* 13(1): 1–19. doi:10.1038/s41598-023-45038-x.
- Burlec, Ana Flavia, Monica H ncianu, Irina Macovei, Cornelia Mircea, Adrian Fifere, Ioana Andreea Turin-Moleavin, Cristina Tuchilu , Silvia Robu, and Andreia Corciov . 2022. "Eco-Friendly Synthesis and Comparative *In vitro* Biological Evaluation of Silver Nanoparticles Using *Tagetes erecta* Flower Extracts." *Applied Sciences (Switzerland)* 12(2). doi:10.3390/app12020887.
- Chikdu;, D., P. Pal;, A. Gujar;, R.; Deshmukh, and S.Kate; 2015. "Green synthesis and characterization of silver nanoparticles by using aloe barbadensis and its antibacterial." *Journal of Global Bioscience* 4(7): 2713–19.
- Devika, K, G Anburaj, R Sathish, and R Manikandan. 2023. "*Tabebuia rosea* (Family Bignoniaceae) Flower Extraction and Its Antioxidant Activity: Green Synthesis of Iron Oxide Nanoparticles Section A-Research Paper *Tabebuia rosea* (Family Bignoniaceae) Flower Extraction and Its Antioxidant Activity: Green Synthesis of Iron Oxide Nanoparticles
- Fatimah, Is. 2016. "Green Synthesis of Silver Nanoparticles Using Extract of *Parkia speciosa* Hassk Pods Assisted by Microwave Irradiation." *Journal of Advanced Research* 7(6): 961–69. doi:10.1016/j.jare.2016.10.002.
- Goudarzi, Mojgan, Noshin Mir, Mehdi Mousavi-Kamazani, Samira Bagheri, and Masoud Salavati-Niasari. 2016. "Biosynthesis and Characterization of Silver Nanoparticles Prepared from Two Novel Natural Precursors by Facile Thermal Decomposition Methods." *Scientific Reports* 6(September): 1–13. doi:10.1038/srep32539.
- Hussain, Zawar, Muhammad Jahangeer, Shafiq Ur Rahman, Tamanna Ihsan, Abid Sarwar, Najeeb Ullah, Tariq Aziz, et al. 2023. "Synthesis of Silver Nanoparticles by Aqueous Extract of *Zingiber officinale* and Their Antibacterial Activities against Selected Species." *Polish Journal of Chemical Technology* 25(3): 23–30. doi:10.2478/pjct-2023-0021.
- Jan, Hasnain, Gouhar Zaman, Hazrat Usman, Rotaba Ansir, Samantha Drouet, Nathalie Gigliolo-Guivarc'h, Christophe Hano, and Bilal Haider Abbasi. 2021. "Biogenically Proficient Synthesis and Characterization of Silver Nanoparticles (Ag-NPs) Employing Aqueous Extract of *Aquilegia pubiflora* along with Their *In Vitro* Antimicrobial, Anti-Cancer and Other Biological Applications." *Journal of Materials Research and Technology* 15: 950–68. doi:10.1016/j.jmrt.2021.08.048.
- Narayanan, Mathiyazhagan, Anburaj Gothandapani, Rajasudha Venugopalan, Manikandan Rethinam, Sakunthala Pitchai, Tahani Awad Alahmadi, Hesham S. Almoallim, Sabariswaran Kandasamy, and Kathirvel Brindhadevi. 2023. "Antioxidant and Anticancer Potential of Ethyl Acetate Extract of Bark and Flower of *Tecoma stans* (Linn) and *In Silico* Studies on Phytoligands against Bcl 2 and VEGFR2 Factors." *Environmental*

- Research 231(May) doi:10.1016/j.envres.2023.116112.
- Ohiduzzaman, Md, M. N.I. Khan, K. A. Khan, and Bithi Paul. 2024. "Biosynthesis of Silver Nanoparticles by Banana Pulp Extract: Characterizations, Antibacterial Activity, and Bioelectricity Generation." *Heliyon* 10(3): e25520. doi:10.1016/j.heliyon.2024.e25520.
- Perumal, P., V. Sekar, V. Rajesh, S. Gandhimathi, R. Sampathkumar, and K. H. Shuja Nazimudin. 2010. "Invitro Antioxidant Activity of *Argemone mexicana* Roots." *International Journal of PharmTech Research* 2(2): 1477–82.
- Rizwana, Humaira, Najat A. Bokahri, Fatimah S. Alkhattaf, Gadah Albasher, and Horiah A. Aldehaish. 2021. "Antifungal, Antibacterial, and Cytotoxic Activities of Silver Nanoparticles Synthesized from Aqueous Extracts of Mace-Arils of *Myristica fragrans*." *Molecules* 26(24). doi:10.3390/molecules26247709.
- Singh, Harjeet, Martin F. Desimone, Shivani Pandya, Srushti Jasani, Noble George, Mohd Adnan, Abdu Aldarhami, Abdulrahman S. Bazaid, and Suliman A. Alderhami. 2023. "Revisiting the Green Synthesis of Nanoparticles: Uncovering Influences of Plant Extracts as Reducing Agents for Enhanced Synthesis Efficiency and Its Biomedical Applications." *International Journal of Nanomedicine* 18(August): 4727–50. doi:10.2147/IJN.S419369.
- Thiyagarajan, Santhanamari, and Subramanian Kanchana. 2022. "Green Synthesis of Silver Nanoparticles Using Leaf Extracts of *Mentha arvensis* Linn. and Demonstration of Their *in Vitro* Antibacterial Activities." *Brazilian Journal of Pharmaceutical Sciences* 58. doi:10.1590/s2175-97902022219898.
- Vidhyasagar, None, Ritu Raj Patel, Sudhir Kumar Singh, and Meenakshi Singh. 2023. "Green Synthesis of Silver Nanoparticles: Methods, Biological Applications, Delivery and Toxicity." *Materials Advances* 4(8): 1831–49. doi:10.1039/d2ma01105k.

**Access this Article in Online**



Website:  
[www.ijcrcps.com](http://www.ijcrcps.com)

Subject:  
Chemistry

Quick Response Code

DOI: [10.22192/ijcrcps.2024.11.03.005](https://doi.org/10.22192/ijcrcps.2024.11.03.005)

How to cite this article:

B. Praveen, R. Manikandan, M. Surendra Varma, G. Anburaj, D. Chinnaraja, C. Sathish Prabu, M. Revathi. (2024). Silver Nanoparticles (AgNPs) characterization of antibacterial and antioxidant properties using *Myristica fragrans* ethanol extract. *Int. J. Curr. Res. Chem. Pharm. Sci.* 11(3): 52-62.  
DOI: <http://dx.doi.org/10.22192/ijcrcps.2024.11.03.005>